Pergamon

Int. J. Mach. Tools Manufact. Vol. 35, No. 10, pp. 1397–1409, 1995

0890-6955/95$9.50 + .00

0890-6955(95)0001-1

APPLIED MECHANICS IN GRINDING—IV. THE MECHANISM OF GRINDING INDUCED PHASE TRANSFORMATION

LIANGCHI ZHANG† and MOFID MAHDI†

(*Received* 22 *September* 1994)

Abstract—One of the most important problems in high precision grinding is the optimisation of the surface residual stress distribution of ground components. It has been realised that the heat generated in the grinding zone plays a central role in the phase transformation of workmaterials that would alter the residual stress formation. The purpose of this paper was to reveal the mechanism of phase transformation of workmaterials induced by grinding. The finite element method was used to simulate the grinding processes. The heat source generated during grinding was considered as a moving heat flux with a triangular profile. Effects of table speed, heat flux distribution, thermal properties of workmaterials and convective features of coolant were discussed in detail. It was found that an optimal combination of grinding conditions could minimise the depth of phase transformation. The results of this paper also offered essential information for the mechanism exploration of residual stresses in ground components.

NOMENCLATURE

D	non-dimensional martensite depth, defined as d/λ
d	depth of martensite zone
H	non-dimensional heat transfer coefficient, defined by $2\alpha h/\kappa v_w$
h	heat transfer coefficient of grinding fluid
L_c	length of a grinding zone, see Fig. 1
l_a	relative apex position of a triangular heat flux, defined as ξ_a/λ
q	heat flux per unit grinding width
q_a	the peak value of the heat flux
q_w	net heat flux per unit grinding width that enters into the workmaterial
$\bar{q}_w$	average value of q_w
Pe	Peclet number, see equation (5)
T	temperature rise relative to the ambient temperature
$\hat{T}$	non-dimensional temperature, defined by equation (5)
T_∞	ambient temperature
v_w	table speed
X, Z	non-dimensional coordinates, see equation (5)
x, z	coordinates, fixed to the workpiece, see Fig. 2
α	thermal diffusivity of the workmaterial
κ	thermal conductivity of the workmaterial
λ	half-length of the grinding zone, i.e. $L_c/2$
ξ, χ	coordinates, fixed to the moving heat source, see Fig. 2
φ	the distribution function of the heat flux, see equations (1) and (2)

1. INTRODUCTION

The phase transformation during grinding would alter the micro-structure and thermal and mechanical properties of the surface layer of a component. Therefore, to ensure a high degree of surface integrity, clarifying the inherent relationships between various grinding conditions and the phase transformation of materials subjected to grinding is of great importance. Fundamentally, there are four problems in the analysis of phase transformation associated with grinding: (1) the strength and distribution of the heat source generated, which relates to the material removal mechanisms of grinding; (2) the convection of cooling media, which reflects the effect of coolant; (3) the thermal properties of the workmaterial, which determines the heat accumulation process and (4) the moving speed of the heat source, which represents the contribution of table

†Centre for Advanced Materials Technology, Department of Mechanical and Mechatronic Engineering, The University of Sydney, NSW 2006, Australia.

speed of a grinding operation. Therefore a full exploration of the realistic effect of key grinding parameters on the extent of phase transformation relies greatly on an adequate modelling of the details of the grinding heat source.

The theory of a moving heat source proposed by Jaeger [1] was the most widely used in the theoretical thermal analysis of grinding. This theory considered that a perfect insulator with a uniformly distributed band heat source was moving at a constant velocity across a semi-infinite stationary body. Applications of this theory were extensive (e.g. [2–6]). However, the theory did not take the cooling effect into account, which is extremely important in a grinding process. Des Ruisseaux and Zerkle [7] extended Jaeger's model to include the effect of surface cooling. The importance of this revision to practical grinding processes was further confirmed by Peters and Vansevenant [8]. In a more detailed consideration of the heat transfer process, Lavine and Jen [9] proposed a physical model to simulate the heat transfer into the wheel, workpiece and grinding fluid. It was also realised experimentally that the surface temperature distribution varied with the rotation directions of the wheel even when all the other grinding conditions were kept the same [10]. This indicated that the profile of the surface heat source would vary with the details of the grinding operations and therefore particular attention should be paid to study the profile effect in the modelling of thermal analysis of grinding [11]. A number of overviews constructed a valuable figure for the recent research progress on the thermal analysis of grinding processes (e.g. [12–15]). Unfortunately, the effect of phase transformation has not been investigated properly so far.

The purpose of this study is to explore the inherent dependence of phase transformation upon grinding conditions. The finite element method is used to simulate the grinding processes. Particular attention has been paid to the effects of heat flux profiles, thermal properties of workmaterial, table speed and the cooling of grinding fluids. Critical conditions for the onset of phase transformation are investigated. This paper, together with the previous parts of the series research, offers essential information for a full understanding of the mechanism of residual stress formation in ground components.

2. MODELLING

2.1. *Problem description*

For a surface grinding process illustrated in Fig. 1, the profile of the heat flux generated in grinding could be approximated by a triangle [11]. The apex, however is located at a point between the inlet and outlet contact points, depending on the particular grinding conditions. In this study, we assume that a band heat source with a triangular profile is moving along the workpiece surface in ξ, x-direction with a constant velocity v_w, which is equal to the grinding table speed in magnitude, see Fig.

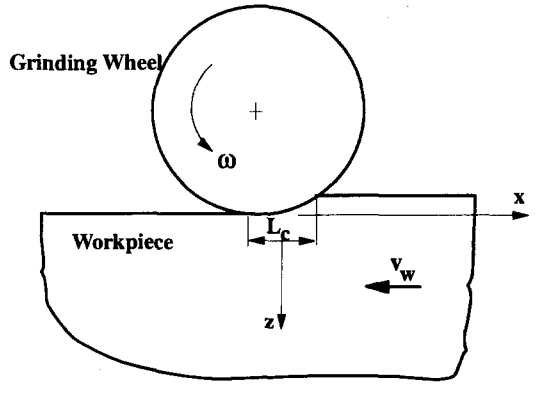

Fig. 1. A schematic diagram of an up-grinding process.

2. The coordinate system $\xi O'\chi$ is fixed to the heat source with its origin O' at the centre of the source and is moving together with it. The coordinate system xOz is fixed to the workpiece and its origin O is coincident with O' at the instant $t = 0$. Letting the apex be at ξ_a and the heat strength per unit grinding width be q, the net heat flux per unit grinding width that enters into the workmaterial could be expressed as

$$q_w = \psi q(\xi) = \psi \bar{q} \phi(\xi) = \bar{q}_w \phi(\xi), \psi < 1 \tag{1}$$

where $\phi(\xi)$ is the distribution function and $\bar{q}_w$ the mean value of q_w. $\psi = 1$ takes place only when all the heat generated during grinding flows by conduction into the workmaterial. For the triangular model used in this study, the distribution function can be expressed as

$$\phi(\xi) = \begin{cases} 0, & \xi \le -\lambda \\ 2\left\{1 + \dfrac{\xi - \xi_a}{\lambda + \xi_a}\right\}, & -\lambda \le \xi \le \xi_a \\ 2\left\{1 - \dfrac{\xi - \xi_a}{\lambda - \xi_a}\right\}, & \xi_a \le \xi \le \lambda \\ 0, & \xi \ge \lambda \end{cases} \tag{2}$$

where $\lambda = L_c/2$ and L_c is the length of the grinding zone that can be calculated by the formula proposed by Zhang *et al.* [16], see Figs 1 and 2. Different ξ_a values could be used for simulating heat sources of different grinding operations, such as up- and down-grinding processes.

The grinding is assumed to be quasi-stationary. Thus the governing differential equation of the induced temperature field in the workmaterial can be written as

$$\frac{\partial^2 T}{\partial x^2} + \frac{\partial^2 T}{\partial z^2} + \frac{v_w}{\alpha}\frac{\partial T}{\partial x} = 0, \tag{3}$$

where T is the temperature rise relative to the ambient temperature T_∞, α the thermal diffusivity of the workmaterial, and x and z are the horizontal and vertical coordinates, see Fig. 1. To take into account the convection induced by the grinding fluid on the workpiece surface (at $z = 0$), the solution of equation (3) must satisfy the following boundary conditions

$$\begin{cases} \kappa \dfrac{\partial T}{\partial z} = \begin{cases} -q_w(x), & |x| \le \lambda, z = 0 \\ hT(x), & z = 0 \end{cases} \\ T, \dfrac{\partial T}{\partial x}, \quad \dfrac{\partial T}{\partial z} \to 0, \quad \text{when } r \to \infty \end{cases} \tag{4}$$

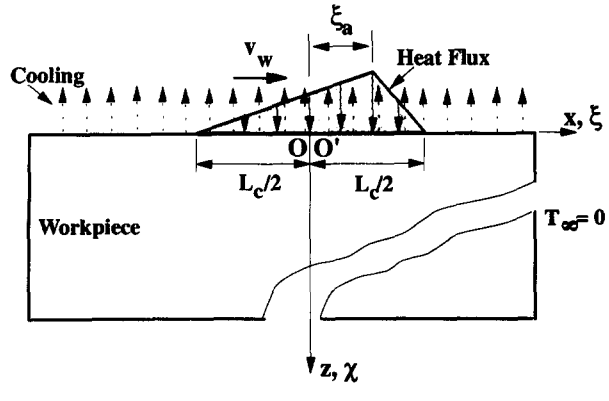

Fig. 2. A model for the thermal analysis of grinding.

where κ is the thermal conductivity of the workmaterial, h the heat transfer coefficient of the grinding fluid and $r = (x^2 + z^2)^{\frac{1}{2}}$. To generalise the analysis, the following non-dimensional parameters and variables are introduced

$$H = \frac{2\alpha h}{\kappa v_w}, X = \frac{v_w x}{2\alpha},$$
$$Z = \frac{v_w z}{2\alpha}, \tag{5}$$
$$Pe = \frac{v_w L_c}{4\alpha}, \bar{T} = \frac{\pi\kappa v_w}{2\alpha q_w} T,$$

where Pe is the well-known Peclet number. Correspondingly, the governing equation (3) and boundary conditions (4) become

$$\frac{\partial^2 \bar{T}}{\partial X^2} + \frac{\partial^2 \bar{T}}{\partial Z^2} + 2\frac{\partial \bar{T}}{\partial X} = 0, \tag{6}$$

and

$$\begin{cases} \dfrac{\partial \bar{T}}{\partial Z} = \begin{cases} -\phi(X), & |X| \le Pe, Z = 0 \\ H\bar{T}(X), & Z = 0 \end{cases} \\ \bar{T}, \dfrac{\partial \bar{T}}{\partial X}, \quad \dfrac{\partial \bar{T}}{\partial Z} \to 0, \quad \text{when } R \to \infty \end{cases} \tag{7}$$

where $R = (X^2 + Z^2)^{\frac{1}{2}}$.

2.2. *Control volume for finite element analysis*

Although the dimension of a workpiece could reasonably be assumed to be semi-infinite in comparison with the small length of the surface heat source, a finite control volume must be applied for the finite element analysis of the boundary value problem specified by equations (6) and (7). The criterion for a proper selection of the dimension of such a control volume is the sufficient accuracy attainable.

For the workmaterial used in this study (the alloy steel AISI-SAE-52100 as listed in Table 1), the most adequate control volume associated with the eight-noded isoparametric finite element of ADINA code [19] is $-3 \le X/Pe \le 2$, $0 \le Z/Pe \le 3$. An error analysis of the surface temperature with this control volume, in comparison with the analytical solutions available [1, 11] for both the rectangular and triangular heat sources, shows that a maximum error less than 6.5% could be guaranteed for all the grinding conditions considered in this study when the above control volume was used.* It is

Table 1. The composition and properties of alloy AISI-SAE-52100 [17, 18]

Composition (% weight)							
C	Mn	S	Cr	α (m^2/sec)	κ (W/m K)	Critical cooling time between 998 K and 773 K (sec)	Austenizing temperature (K)
0.94	0.34	0.27	0.95	1.13×10^{-5}	42.7	<2.155	1048

*The mesh was uniform across the control volume but the element number for the problems associated with different Pe values were different. The number of elements used was $N_z \times N_x = 20 \times 20$ (= 400) for Pe = 1, 20×40 (= 800) for Pe = 2, 3 and 20×80 (= 1600) for Pe = 4, where N_z denotes the element number in Z-direction and N_x is that in X-direction in the control volume.

very much acceptable in engineering practice. The relative error distributions for different Pe and l_a and different types of heat sources are exhibited in Fig. 3, where $l_a = \xi_a/\lambda$ is the relative position of the apex of the triangular heat flux. A typical value of a grinding zone length of 2 mm was used throughout the calculations. In the cases of constant input heat fluxes, the maximum absolute error decreases as Pe increases. This means that a low table speed yields more heat diffusion in the grinding direction and hence a relatively larger control volume may be used, if a further accuracy improvement is required. On the other hand, the cases with triangular input heat fluxes show that decreasing l_a yields larger errors at the left boundaries of the control volume. This indicates that the heat diffusion is more significant in the moving direction of the heat source.

3. RESULTS AND DISCUSSION

3.1. *Temperature distribution*

It was reported that the temperature distribution depends on the details of a particular grinding operation [10]. For instance, up- and down-grinding would give rise to different surface temperature distributions even if all the other conditions were kept the same, see Fig. 4.

The surface temperature distributions associated with different input heat fluxes state that different types of grinding operations could be simulated by changing the apex position of the heat flux, see Fig. 5. According to the deformation mechanism revealed by our previous studies [20], the apex position of the heat flux, l_a, must vary in the

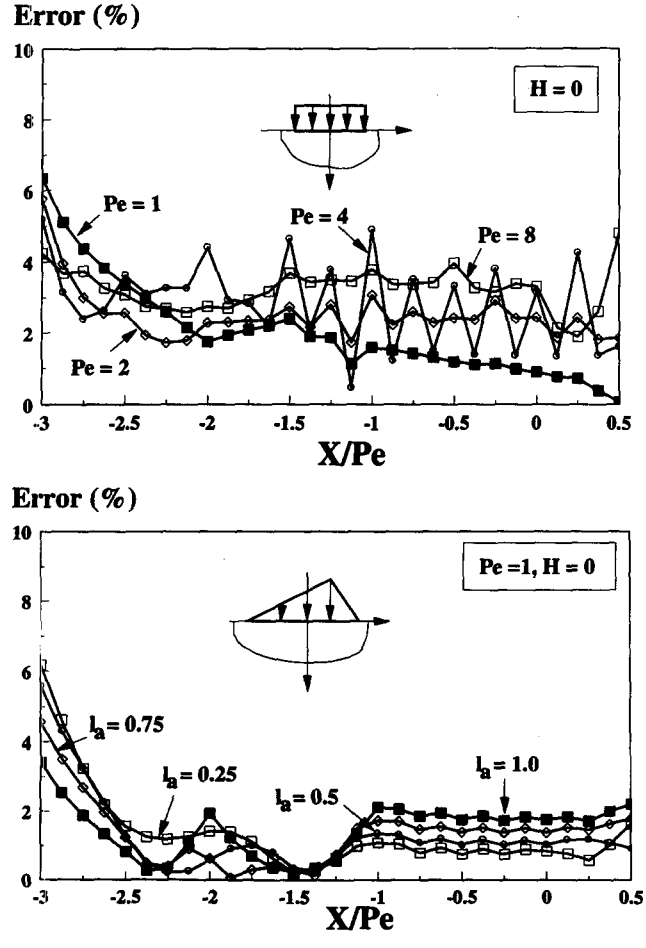

Fig. 3. Error distribution: (a) with a rectangular heat source and (b) with triangular heat sources.

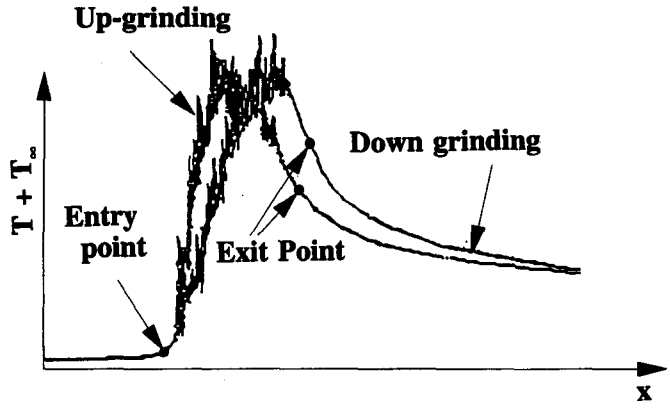

Fig. 4. Effect of types of grinding operations [10].

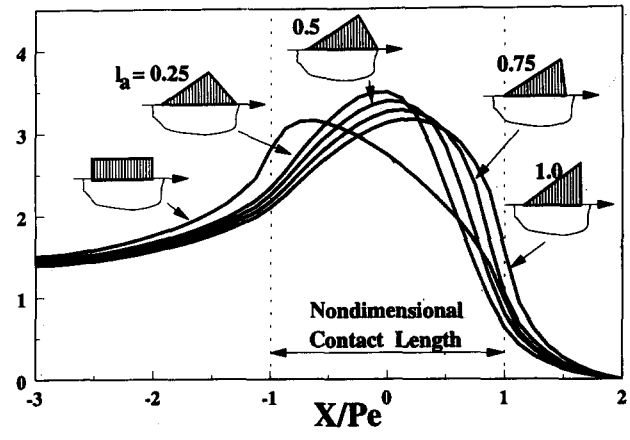

Fig. 5. Variation of surface temperature distribution with the heat flux profile.

range of (0, 1) for either conventional or creep-feed grinding processes. Compared with creep-feed grinding, the table speed of a conventional grinder is much higher and the wheel depth of cut much smaller. With the theory of interface deformation proposed [20], therefore, the distance of the peak of the contact forces from the centre of the contact length between the wheel and workpiece, and hence the l_a value of the heat flux for a conventional grinding operation must be smaller. As we will see in the next section, the change of the surface temperature distribution caused by the variation of l_a (Fig. 5) will significantly influence the process of phase transformation.

Figure 6 shows the variation of the temperature field inside a workpiece with the change of the heat transfer coefficient, or in other words, with the change of the types of grinding fluids. Clearly, a larger H thins down the high temperature zone rapidly and localises the temperature rise significantly. From the figure, it can be seen that even the surface temperature rise inside the grinding zone has been decreased to a great extent. However, it was assumed in equations (4) and (7) that a constant cooling rate exists over the whole surface of the workpiece. Accordingly, if the cooling condition inside the grinding zone is not as assumed, the real surface temperature rise will be higher than the present prediction. On the other hand, the localisation of the temperature field indicates the variation of cooling rate inside the workmaterial. This must have a large effect on the process of phase transformation and we will discuss it in the relevant sections below.

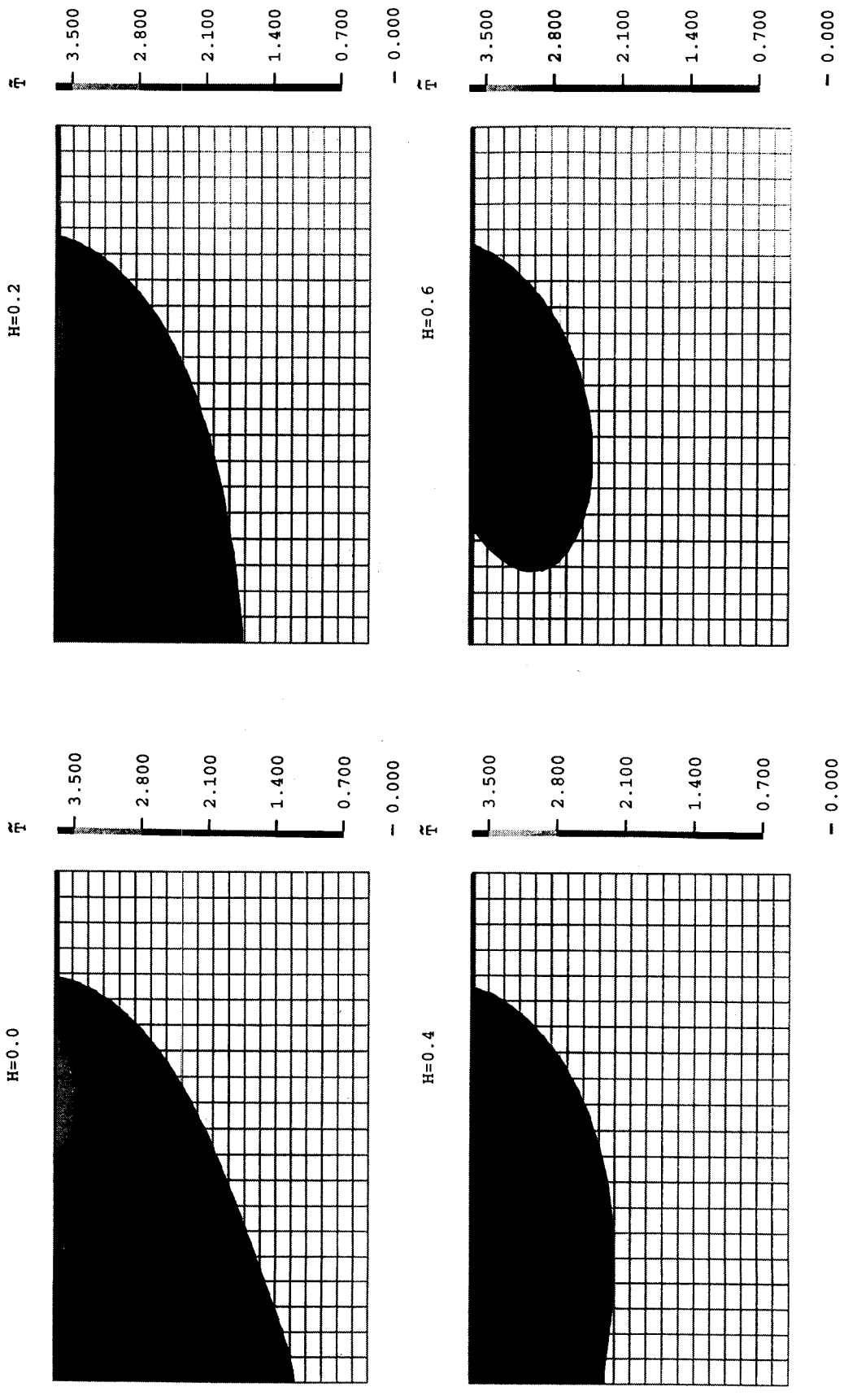

Fig. 6. Effect of cooling on the temperature field inside the workmaterial ($l_a = 0.25$, $Pe = 1$).

3.2. *Phase transformation*

The Peclet number Pe, apex position of heat flux l_a, heat transfer coefficient H and the magnitude of the heat flux q_a, are found to be the most important parameters that affect the grinding induced phase transformation. According to their definitions specified by equations (1), (2) and (5), Pe indicates the effect of table speed, l_a reflects the different types of grinding operations, H represents the cooling property of grinding fluids and q_a indicates the heat conducted into the workmaterial.

Figure 7 demonstrates the variation of the non-dimensional martensite depth D with H, q_a and l_a when Pe is specified. For a given l_a and q_a, D decreases rapidly with the increase of H, that is, a higher cooling rate produces a thinner martensite layer. This is because the phase transformation of a material needs time, that is, to have phase transformation a time interval is required for changing the temperature to a critical level, but a large H shortens such a time interval remarkably. It would become much clearer if the above discussion on the variation of the temperature field in the workmaterial is recalled. On the contrary, increasing q_a offers more time for phase transformation and hence leads to a larger martensite depth. However, if the corresponding cooling is not sufficient as q_a increases, the material will be molten. For given Pe, H and q_a, decreasing l_a increases the martensite depth. This means that moving the apex of the heat flux towards the centre of the grinding zone makes the cooling process slower. Thus a conventional grinding process facilitates martensite transformation in this sense, and an up- and down-grinding operation will produce different depths of martensite even when the other conditions are the same.

The Peclet number has a big effect on the process of phase transformation, see Fig. 8 in comparison with Fig. 7. For a larger Pe, and thus a larger table speed, the phase transformation requires a higher heat input. In practice, the heat generated during grinding is a monotonic increasing function of the material removal rate. Therefore, if the wheel depth of cut is a constant, the heat generated would be the function of table speed only. An increment of the Peclet number would therefore produce more heat and in turn cause a possible phase transformation. It should be noted that the martensite depth is usually much smaller and its variation with H much steeper in the case of a large table speed according to the prediction of Fig. 8. This is because a large Pe shortens the process of heat accumulation in the workmaterial, see Fig. 6, and accordingly thins down the depth of martensite zone and increases the slope of D curves with respect to H. It then follows, from the different features of conventional and creep-feed grinding operations, that conventional grinding processes would usually bring about thinner martensite layers.

The boundary between the molten and solid zones of the present alloy is always a straight line as illustrated in Figs 7 and 8. When Pe is small, the variation of this boundary is not remarkable with respect to the change of l_a and H, see, for instance, the case with $Pe = 1$ in Fig. 7. As Pe increases, the dependence of the boundary on l_a and H becomes stronger (Fig. 8). This is partly due to the localisation effect of the temperature field shown in Fig. 6.

It is of interest to note that the variation of martensite depth D with l_a also relates to the magnitude of H for a constant table speed (i.e. Pe given) and q_a, as shown in Fig. 9. D decreases when l_a varies from 0.25 to 0.5 and from 0.75 to 1. However, in the interval of $l_a \in (0.5, 0.75)$, D would increase for small H, remain constant for intermediate H and decrease for large H. Moreover, small H results in more significant change of D. It is determined by the complex process of heat conduction and accumulation in the workmaterial and the time duration allowed for phase transformation for different H values. Figure 10 demonstrates more straightforwardly the variation of D in the workmaterial. When l_a is smaller, the distance between the onset point of the martensite layer and the moving heat flux is shorter. Thus a smaller l_a corresponds to an earlier initiation of phase transformation.

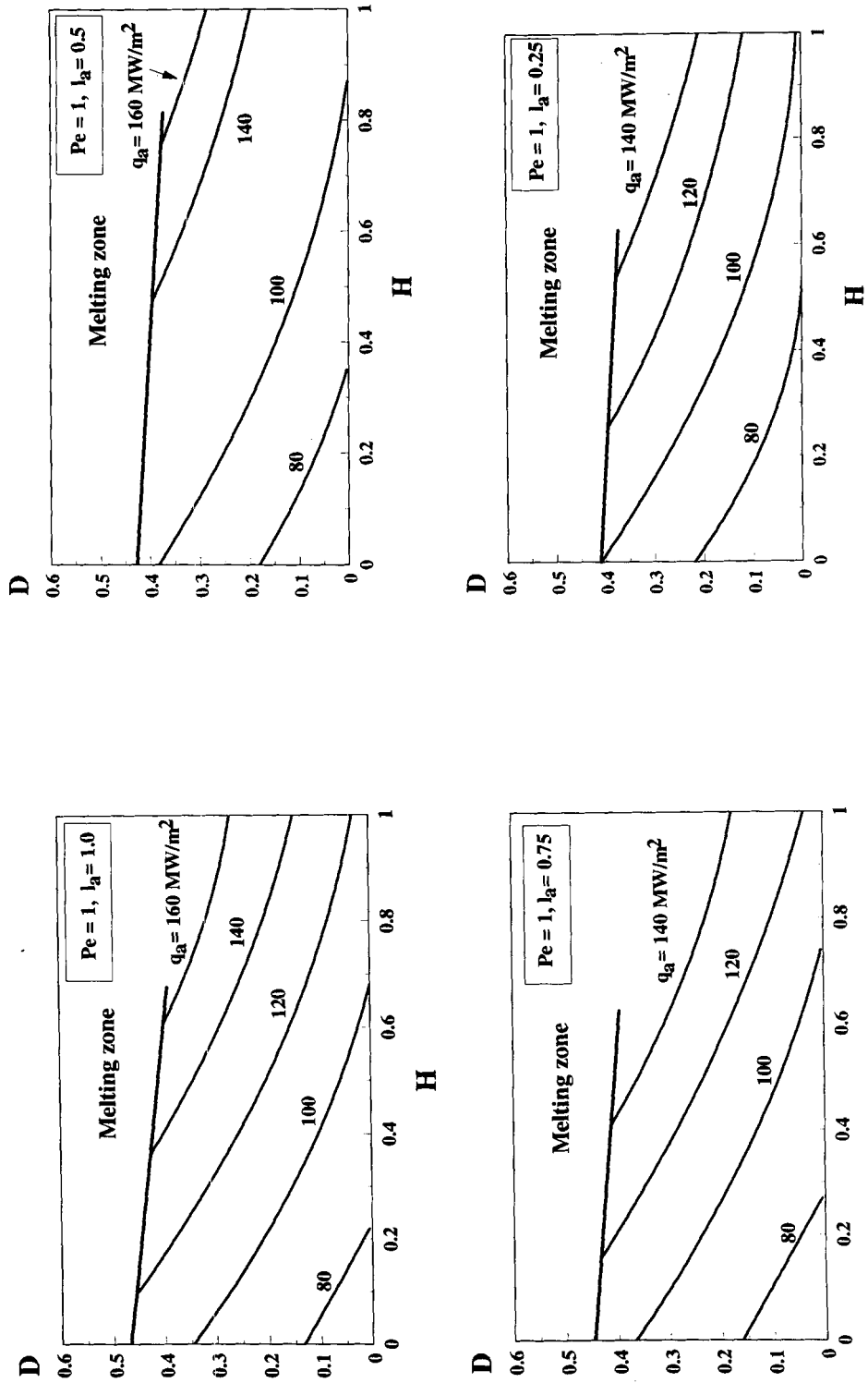

Fig. 7. Variation of martensite depth with H and l_a.

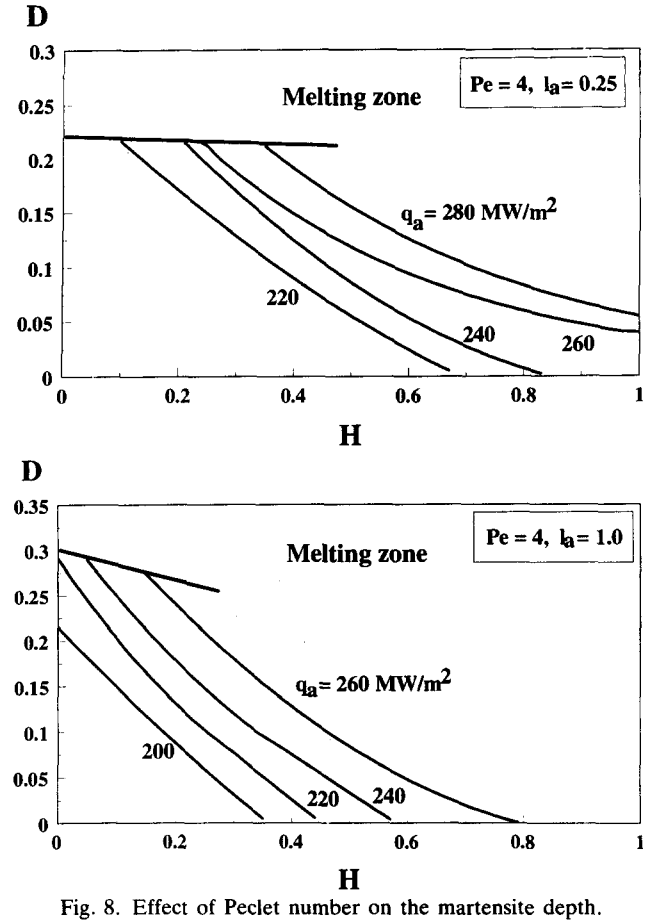

Fig. 8. Effect of Peclet number on the martensite depth.

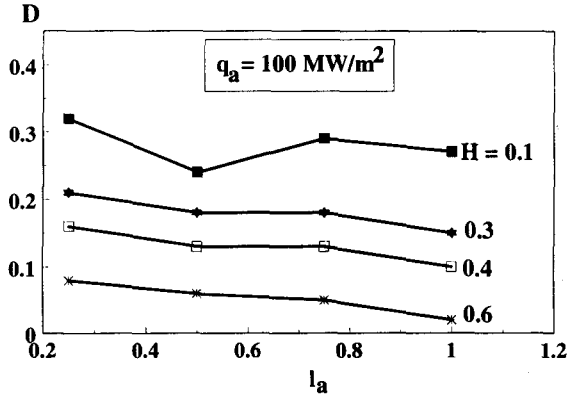

Fig. 9. Influence of l_a.

3.3. *Critical grinding conditions for phase transformation*

The critical grinding conditions are those under which a phase transformation initiates. Figure 11 predicts the critical curves for the onset of martensite transformation. Increasing the table speed requires more heat input for the initiation of martensite. With a smaller l_a, i.e. the peak of the heat flux being closer to the centre of the grinding zone, the onset of phase transformation requires a lower heat input for a given H. In other words, the type of grinding operations, up- or down-grinding for instance, would

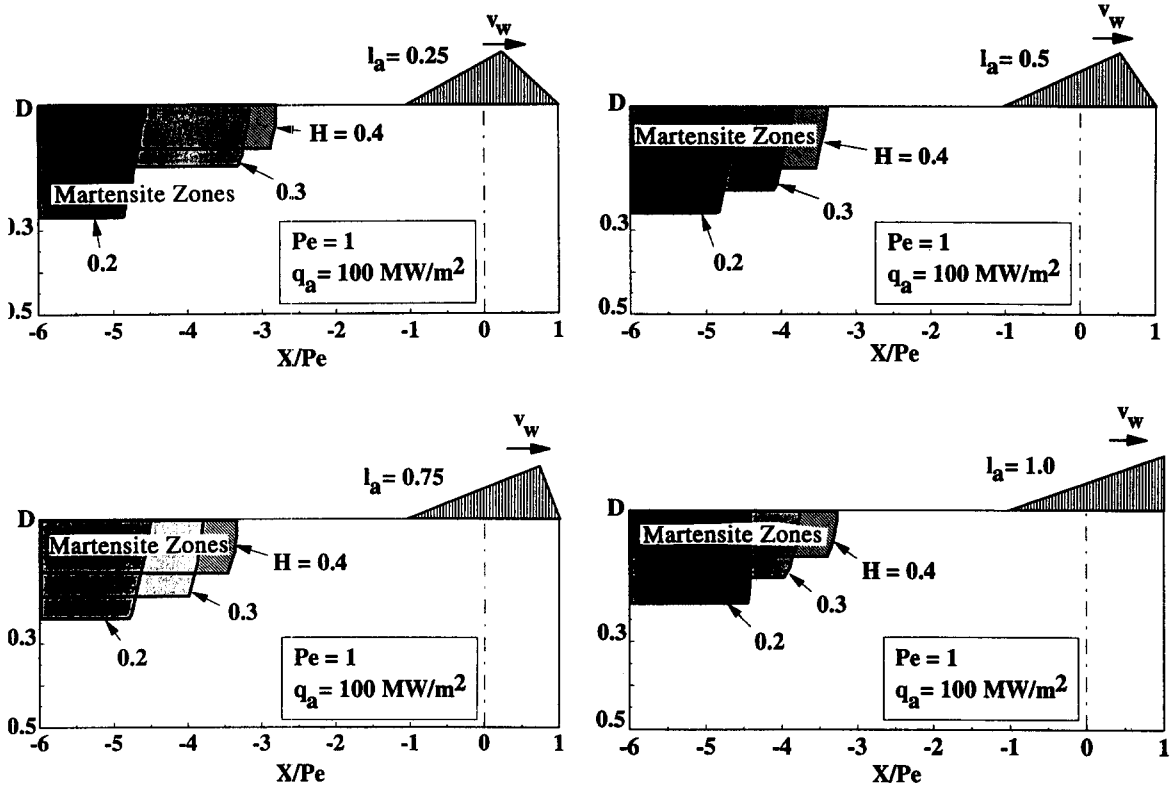

Fig. 10. Distribution of martensite zones.

alter the requirement of q_a even when all the other grinding conditions are the same (Fig. 11a). Cooling is the most important factor here, which is indicated by the slopes of the critical curves. The effect of l_a becomes significant when H is larger (Fig. 11b). A comprehensive analysis of Fig. 11 leads to an approximate formula for estimating the onset of martensite transformation:

$$q_a = a + b\zeta + c\zeta^2 , \tag{8}$$

where

$$\zeta = (1 + H)^{\alpha_1} (Pe)^{\alpha_2} (l_a)^{\alpha_3} , \tag{9}$$

where $a = 55.4$, $b = 14.9$, $c = 3.47$, $\alpha_1 = 0.900$, $\alpha_2 = 0.900$ and $\alpha_3 = 0.075$. A master curve can be obtained if all the critical conditions are plotted under the coordinate system $q_a \sim \zeta$, as shown in Fig. 12. Therefore, ζ defined by equation (9) could be considered as a key non-dimensional parameter of studying the grinding induced phase transformation. Figure 12 can easily be used to find the corresponding critical q_a when H, Pe and l_a are known. If $H = 0$, ζ will involve Pe and l_a only. This indicates a dry grinding process. Similar diagrams to Fig. 12 could be developed for different materials.

4. CONCLUSIONS

The mechanism of phase transformation induced by grinding has been investigated carefully. The dependence of phase transformation upon grinding conditions has been explored. Specifically, the following conclusions are of importance:

(1) The heat transfer coefficient H, Peclet number Pe and the apex position of the heat flux l_a are the main governing grinding parameters affecting the phase transformation in a ground component. In other words, the type of grinding fluid, table speed

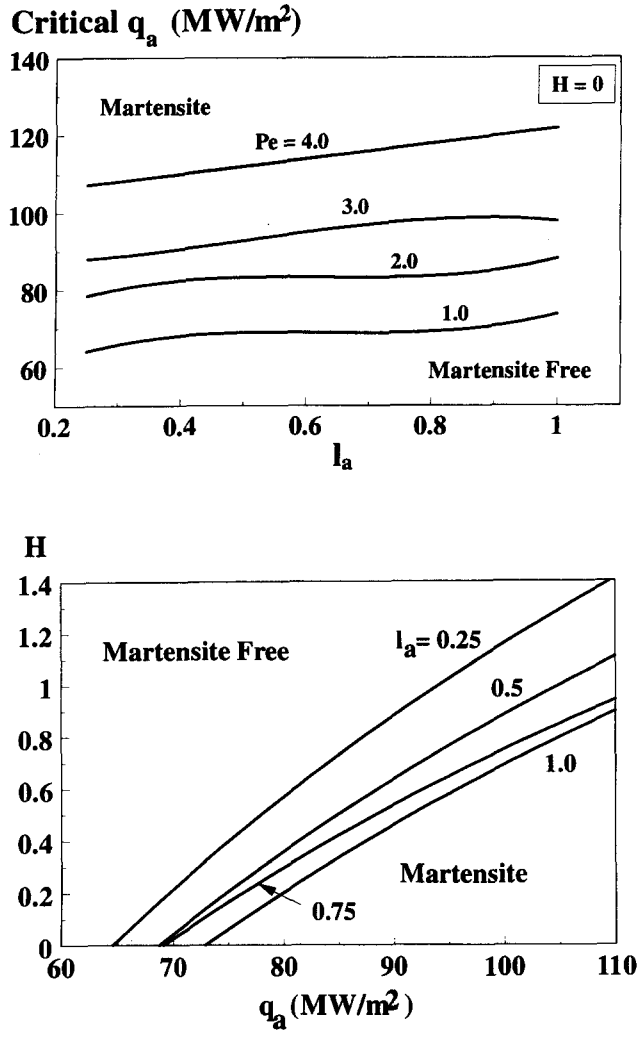

Fig. 11. Critical curves for the onset of martensite transformation.

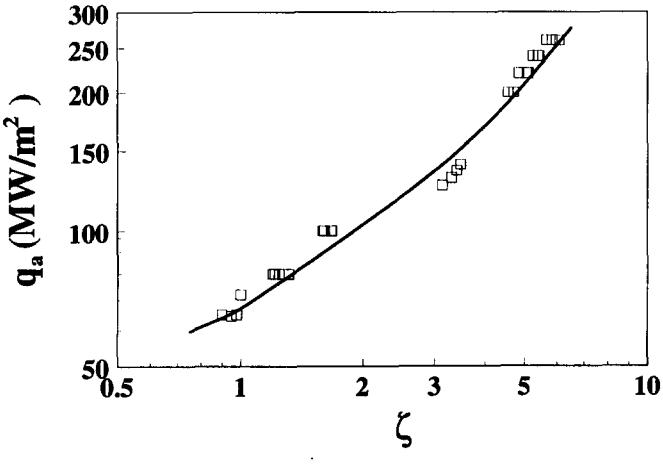

Fig. 12. The master curve for predicting the phase transformation.

and type of grinding operations should be taken into account if the surface phase transformation in a ground component is a main concern.

(2) A relationship, equation (9), between the input heat parameter q_a and the dominant grinding parameters exists. The master curve developed is useful for predicting critical grinding conditions. Similar relations may be developed for different materials.

(3) Compared with a conventional grinding process, a creep-feed grinding operation would produce a larger depth of surface phase transformation.

Acknowledgements—This study was supported by ARC Small Grant. ADINA code was used for all the calculations.

REFERENCES

[1] J. C. Jaeger, Moving sources of heat and the temperature at sliding contacts, *Proc. R. Soc. New South Wales* **76**, 203–224 (1943).
[2] N. R. Des Ruisseaux and R. D. Zerkle, Thermal analysis of the grinding process, *Trans ASME J. Engng Ind.* **92**, 428–434 (1970).
[3] J. O. Outwater and M. C. Shaw, Surface temperature in grinding, *Trans ASME* **74**, 73–86 (1952).
[4] S. Malkin, Thermal aspects of grinding—II. Surface temperatures and workpiece burn, *Trans. ASME J. Engng Ind.* **96**, 1184–1191 (1974).
[5] M. C. Shaw, Temperatures in cutting and grinding, *ASME Heat Transfer Div.* **146**, 17–24 (1990).
[6] M. C. Shaw, The Galileo Principle, *Ann. CIRP* **41**(1), 393–396 (1992).
[7] N. R. Des Ruisseaux and R. D. Zerkle, Temperature in semi-infinite and cylindrical bodies subjected to moving heat sources and surface cooling, *Trans. ASME J. Heat Transfer* **92**, 456–464 (1970).
[8] J. Peters and E. Vansevenant, A thermal model covering pendulum grinding and creep feed grinding, *Ann. CIRP* **32**(1), 491–494 (1983).
[9] A. S. Lavine and T.-C. Jen, Thermal aspects of grinding: heat transfer to workpiece, wheel, and fluid, *Trans. ASME J. Heat Transfer* **113**, 296–303 (1991).
[10] J. G. Wager and D. Y. Gu, Influence of up-grinding and down-grinding on the contact zone, *Ann. CIRP* **40**(1), 323–326 (1991).
[11] L. C. Zhang, T. Suto, H. Noguchi and T. Waida, On some fundamental problems in grinding, in *Computer Methods and Experimental Measurements for Surface Treatment Effects* (edited by M. H. Aliabadi and C. A. Brebbia), pp. 275–284. Computational Mechanics Publications, Southampton, U.K. (1993).
[12] C. Andrew, T. D. Howes and T. R. A. Pearce, *Creep Feed Grinding*. Industrial Press, New York (1985).
[13] S. Malkin, *Grinding Technology: Theory and Applications of Machining with Abrasives*. Ellis Horwood, New York (1989).
[14] W. B. Rowe, M. N. Morgan and D. A. Allanson, An advance in the modelling of thermal effects in the grinding process, *Ann. CIRP* **40**(1), 339–342 (1991).
[15] L. C. Zhang, T. Suto, H. Noguchi and T. Waida, An overview of applied mechanics in grinding, *Manufact. Rev.* **5**(4), 261–273 (1992).
[16] L. C. Zhang, T. Suto, H. Noguchi and T. Waida, Applied mechanics in grinding, Part III: a new formula for contact length prediction and a comparison of available models, *Int. J. Mach. Tools Manufact.* **33**(4), 589–597 (1993).
[17] ASM Handbook Committee, *Metals Hand Book—Properties and Selection: Iron and Steels*, Vol. 4, pp. 145–149, 9th edition. American Society of Metals, Ohio, U.S.A. (1981).
[18] M. Atkin, *Atlas of Continuous Cooling Transformation Diagram for Engineering Steels*, pp. 227–229. British Steel Corporation, Sheffield, U.K. (1977).
[19] ADINA R&D Inc., User's Manual, Version 6.1 (1992).
[20] L. C. Zhang, T. Suto, H. Noguchi and T. Waida, Applied mechanics in grinding—II. Modelling of elastic modulus of wheels and interface forces, *Int. J. Mach. Tools Manufact.* **33**(2), 245–255 (1993).